

# Self-Calibrating Radial Generalized SENSE

R. Bammer<sup>1</sup>, K. K. Vigen<sup>1</sup>, K. P. Pruessmann<sup>2</sup>, M. Markl<sup>1</sup>, M. E. Moseley<sup>1</sup>

<sup>1</sup>Radiology, Stanford University, Stanford, CA, United States, <sup>2</sup>ETH and University of Zurich, Zurich, Switzerland

**Introduction:** The initial parallel imaging approaches utilized a separate calibration scan to estimate the coil sensitivity for image reconstruction<sup>1,2</sup>. However, the need for the acquisition of a separate calibration scan is unfortunate, since it requires additional scan time and may be erroneous due to motion. The latter consideration is especially important for free-breathing real-time cardiac studies where large dynamic excursions of the thorax and the internal organs can be anticipated. Trajectories that excessively sample the k-space origin, such as variable density spirals or radial, provide inherent calibration capabilities if the critically sampled portion around the center of the k-space is used. Variable-density cartesian and spiral trajectories have been presented earlier for auto-calibration purposes<sup>3,4</sup>. Here, we will investigate the properties of radial trajectories and their capabilities of very high reduction factors.

**Methods:** Axial 2D balanced FFE (MFAST) and 3D SPGR sequences were implemented on a commercially available MRI 1.5T unit (Signa CV/i, GE Medical Systems, Waukesha, WI) with high performance gradients (40 mT/m,  $t_{rise} = 268\mu s$ ) and a four element cardiac array coil for parallel imaging acquisition. All procedures were approved by the institutional review board of our institution. For both sequences radial readout trajectories were used with undersampling in the azimuthal dimension. Conventional Cartesian encoding was used along the slice direction for the 3D SPGR sequence. The scan parameters were as follows: *3D-SPGR*: FOV=22cm, slice thickness=4mm, reconstruction matrix = 256x256,  $\alpha=25$ , TR/TE=30/12ms, slices = 28, number of radial projections = 256; *2D-MFAST*: FOV=22cm, slice thickness=4mm, reconstruction matrix = 256x256,  $\alpha=50$ , TR/TE=5/2ms, slices = 1, number of radial projections = 256. Reduction factors from R=1 (256 projections) to R=16 (16 projections) were investigated. Image reconstruction was conducted in two steps using an iterative generalized SENSE (GSENSE) algorithm<sup>5</sup>. In the first step only the central part of k-space (that fulfilled the Nyquist sampling rate) was reconstructed to generate a low-resolution image for each component coil. The individual component coil images and their sum-of-squares reconstruction were used to calculate the coil sensitivity maps for the second reconstruction step. Here, the complete data set (entire k-space) underwent the iterative GSENSE algorithm with typically 6 to 25 iterations.

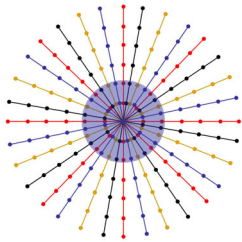


**Figure 1 – Schematic radial trajectory.** The radial k-space trajectory intrinsically has a variable k-space sampling density pattern, where critically sampled k-space portions usually occur at the edges of k-space, whereas the center of k-space is excessively oversampled (shaded area). Hence, from the central k-space region low-resolution images can be reconstructed without azimuthal aliasing.

**Results:** Figure 2 shows a side-by-side comparison between a phantom scanned using a regular birdcage coil or a four element array coil with GSENSE reconstruction at different reduction factors (R=2, 6, 8, and 16). While typical streaking artifacts are already slightly apparent at R=2 for the conventional radial reconstruction, for the GSENSE reconstruction streaking became significant only at higher reduction factors (R>14).

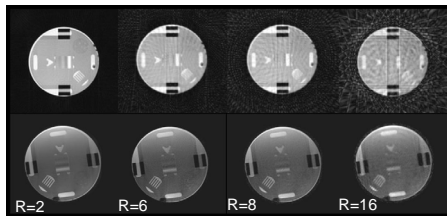


**Figure 2 – Conventional gridding vs. GSENSE reconstruction.** (top row) Conventional gridding-reconstruction of radial data obtained with a birdcage coil at reduction factors of (R=2,6,8, and 16). (bottom row) Corresponding GSENSE reconstruction using four coils attached symmetrically around the circumference of the phantom. To obtain a sensitivity estimate, the center portion (~20x20) of the k-space was initially reconstructed to form a low-resolution image.

Figure 3 shows another side-by-side comparison between conventional gridding-reconstruction and the GSENSE reconstruction using the same axial 3D-SPGR data set. This figure clearly demonstrates the great reduction of streaking artifacts with the GSENSE reconstruction. A close up view of Figure 3 (Fig. 4) allows a better appreciation of residual reconstruction artifacts. From Figure 4 it is apparent that for  $R > 4$  image degradation occurs (c.f. vessels in the sylvian fissure). Notice, however, that the number of projections chosen for our R=1 already implies azimuthal undersampling of radial data by the Nyquist criterion. Since the coil sensitivity estimates are calibrated using a sum-of-squares reconstruction, the image non-uniformities are also apparent in the final GSENSE reconstructions. At very high reduction factors ( $R > n_{coils}$ ) the GSENSE reconstruction was not able to fully fill in the highest frequency information that was left out due to the undersampling procedure. As a consequence, in this reduction range, the amount of streaking artifacts was reduced at the cost of apparent spatial resolution.

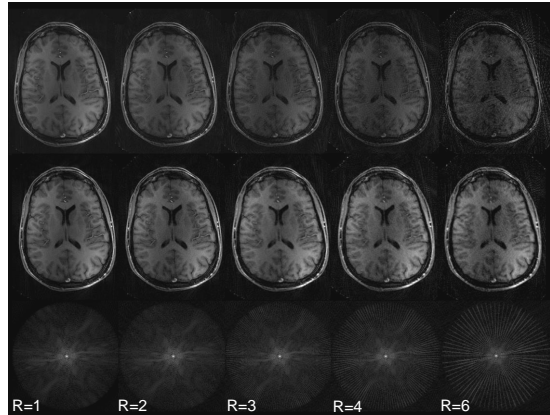


**Figure 3 – Radial 3D-SPGR.** (top row) Conventional gridding- and sum-of-squares reconstruction of radial data from a four element array coil at reduction factors of (R=1,2,3,4, and 6). Again, the four coils were attached symmetrically around the circumference of the subject's head. (middle row) Corresponding GSENSE reconstruction. (bottom row) Initially gridded k-space data for one coil element.

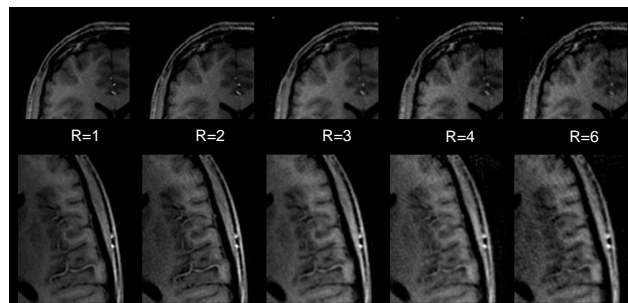


**Figure 4 – Close up view.** View of the right frontal lobe and the left sylvian fissure from the GSENSE reconstructions (R=1,2,3,4, and 6) shown in Fig. 3.

**Discussion:** Radial k-space trajectories excessively oversample the k-space origin and provide higher resolution per unit time than Cartesian imaging<sup>6</sup>. Hence, they are inherently suited for autocalibration in generalized SENSE reconstructions and therefore of great advantage in the presence of bulk physiologic motion, where conventional calibration scans can be unreliable. Using the GSENSE reconstruction our phantom experiments showed only minimal distortions even for  $R \gg n_{coils}$ . However, these high reduction factors could not be reproduced *in vivo*. This is likely linked to the larger proportion of the head relative to the FOV, the size and arrangement of the coil elements, and lower SNR in the *in vivo* experiments. Nevertheless, for *in vivo* applications GSENSE allows one to take advantage of significant azimuthal sampling reductions ( $R \sim n_{coil}$ ). At higher reduction factors ( $R \gg n_{coils}$ ), the diminished level of streaking artifacts appeared to be traded for spatial resolution.

**References:** <sup>1</sup>Sodickson DK, et al. MRM 38: 591-603, 1997. <sup>2</sup>Pruessmann KP, et al. MRM 42: 952-62, 1999. <sup>3</sup>Jakob PM, et al. MAGMA 7: 638-51, 1998. <sup>4</sup>McKenzie CA, et al. Minimum Data Acquisition Methods: p178-81, 2001. <sup>5</sup>Pruessmann KP, et al. MRM 46: 638-51, 2001. <sup>6</sup>Peters DC, et al. MRM 43: 91-101, 2000. **Acknowledgements:** This work was supported in part by the NIH (1R01EB002771, 1R01NS35959), the Center of Advanced MR Technology at Stanford (P41RR09784), and the Lucas Foundation.